Geometric Analysis of the Kinematic Sensitivity of Planar Parallel Mechanisms

M. H. Saadatzi[1],　M. Tale Masouleh[2],　H. D. Taghirad[1],　C. Gosselin[2],　P. Cardou[2]

[1]*Advanced Robotics & Automated Systems (ARAS), Faculty of Electrical & Computer Engineering, K.N. Toosi University of Technology, P.O. Box 16315-1355, Tehran, Iran, saadatzi@ee.kntu.ac.ir, Taghirad@kntu.ac.ir*
[2]*Laboratoire de robotique, Département de génie mécanique, Université Laval - Québec, QC, Canada - G1V 0A6, mehdi.tale-masouleh.1@ulaval.ca, Clement.Gosselin@gmc.ulaval.ca, pcardou@gmc.ulaval.ca*

Abstract

The kinematic sensitivity is a unit-consistent measure that has been recently proposed as a mechanism performance index to compare robot architectures. This paper presents a robust geometric approach for computing this index for the case of planar parallel mechanisms. The physical meaning of the kinematic sensitivity is investigated through different combinations of the Euclidean and infinity norms and by means of several illustrative examples. Finally, this paper opens the avenue to the dimensional synthesis of parallel mechanisms by exploring the meaning of the global kinematic sensitivity index.

Keywords: Performance index, kinematic sensitivity, planar parallel mechanisms, redundant mechanisms, mechanisms with dependent degrees of freedom.

Analyse Géométrique de la Sensibilité Cinématique des Mécanismes Parallèles Plans

Résumé

La sensibilité cinématique a été proposée récemment comme un indice de performance pour comparer les architectures des robots en fonction de leurs propriétés cinématiques. Cet article présente une approche géométrique robuste pour calculer la sensibilité cinématique des mécanismes parallèles plans en incluant exemples illustratifs. Dans cet article, la sensibilité cinématique est étudiée par une combinaison des normes euclidienne et infinie afin d'obtenir la combinaison la plus sensée, d'un point de vue physique. En outre, cet article ouvre des pistes pour la synthèse dimensionnelle des mécanismes parallèles en explorant la signification de l'indice de sensibilité cinématique globale.

Mots-clé: Indice de performance, sensibilité cinématique, mécanismes parallèles plans, mécanismes parallèles redondants, mécanismes parallèles avec des degrés liberté dépendants.

1 INTRODUCTION

The definition of sound general performance indices for mechanisms, including Parallel Manipulators (PMs), has received much attention from the robotics research community [1]. This is due to need to compare different robot architectures [2]. As reviewed in [1], the most notorious indices, namely, the manipulability and the dexterity, still entail some drawbacks [1, 3–5], due to the impossibility of defining a single invariant metric for the special Euclidean group. In [1], two distinct metrics are proposed: one for rotations and one for point displacements. They are referred to as the kinematic sensitivity indices. These indices provide tight upper bounds of the magnitudes of the end-effector rotations and point–displacements, respectively, under a unit–magnitude array of actuated–joint displacements [1].

Hence, the maximum kinematic sensitivity is defined as the maximum error that occurs in the Cartesian workspace as a result of bounded displacements in the joint space. In order to obtain consistent unit, two indices have been defined [1]:

$$\sigma_{r_{c,f}} \equiv \max_{\|\boldsymbol{\rho}\|_c=1} \| \boldsymbol{\phi} \|_f, \text{ and } \sigma_{p_{c,f}} \equiv \max_{\|\boldsymbol{\rho}\|_c=1} \| \mathbf{p} \|_f, \tag{1}$$

where, $\boldsymbol{\phi}$ is the array of small rotations of the end–effector about the Cartesian axes, $\mathbf{p}$ represents a small displacement of the operation point, and $\boldsymbol{\rho}$ is the array of small actuator displacements. These two indices are referred to as the maximum rotation and point–displacement sensitivities, respectively. In [1], the definitions of the kinematic sensitivity for serial and parallel mechanisms are based on the same norm in the constraint and the objective functions, i.e., $c = f$. Obviously, different norms for the constraint and objective functions of the kinematic sensitivity lead to different indices with different interpretations. This paper aims at investigating and comparing these different indices, in order to end up with the most meaningful index for planar parallel mechanisms. As a case study, emphasis will be placed on the 3-R$\underline{P}$R parallel mechanism, which is considered a representative example of planar parallel mechanisms in general.

Merlet in [6], concluded that the calculation of the mechanism performance indices must be done while considering independent joint displacements, which immediately leads to $c = \infty$. The results of this paper confirm this conclusion, and, moreover, provide some new observations and interpretations on the use of different norms in the kinematic sensitivity indices. This paper also extends and reviews the approach and routines used in [1] for $c = f = 2$, which leads to some interesting closed–form solutions, and for $c = f = \infty$, using linear programming.

The remainder of this paper is organized as follows. First, the formulation used in [1] for the Jacobian matrix of parallel mechanisms is reviewed. Then, the methods of computation of the kinematic sensitivity for different combinations of Euclidean and ∞ norms are detailed, and illustrated through typical examples for parallel mechanisms. The paper extends the study by presenting the kinematic sensitivity as a global performance index of the mechanism, and, finally, concluding remarks are given to provide more insight into ongoing research.
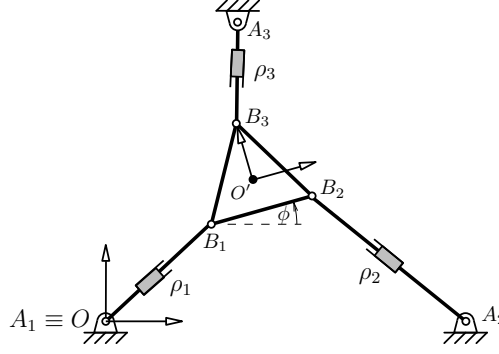
Figure 1: Schematic representation of a planar 3-R<u>P</u>R parallel mechanism.

2   KINEMATIC SENSITIVITY OF FULLY-PARALLEL MECHANISMS

Differentiating the loop–closure equations of a parallel mechanism results in its first-order kinematics relationship, which can be formulated as follows [1]:

$$\boldsymbol{\rho} = \mathbf{K}_p \mathbf{p} + \mathbf{K}_r \boldsymbol{\phi}, \qquad (2)$$

in which, $\boldsymbol{\rho} \in \mathbb{R}^n$ represents small actuator displacements and $\mathbf{x} = [\mathbf{p}^T, \boldsymbol{\phi}^T]^T$ stands for the operation-point position and the orientation, i.e., the pose, of the end–effector. Moreover, consider $\mathbf{K}_p \equiv [\mathbf{k}_1, \mathbf{k}_2, \mathbf{k}_3]$, $\mathbf{K}_r \equiv [\mathbf{k}_4, \mathbf{k}_5, \mathbf{k}_6]$ and $\mathbf{K} \equiv [\mathbf{K}_p, \mathbf{K}_r]$. In parallel manipulators, according to Eq. (2), constraint $\parallel \boldsymbol{\rho} \parallel_c \leq 1$ may be rewritten as $\parallel \mathbf{Kx} \parallel_c \leq 1$, which represents the set of possible pose errors for unit bounds of the (small) actuator displacement errors. $\parallel \mathbf{Kx} \parallel_\infty \leq 1$ and $\parallel \mathbf{Kx} \parallel_2 \leq 1$ can be geometrically represented by a polyhedron and ellipsoid in $\mathbb{R}^6$, respectively. These geometric interpretations are used in this paper to compute the kinematic sensitivity of the mechanisms under study.

2.1   Kinematic sensitivity in the case for which $c = \infty$ and $f = \{2, \infty\}$

The constraint $\parallel \mathbf{Kx} \parallel_\infty \leq 1$ represents a zonotope in $\mathbb{R}^6$. Since the objective functions of Eq. (1) are both convex functions to be maximized, the optimum is bound to occur at a vertex of the zonotope. The maximum objective value among all vertices are labelled $\sigma_{r_{\infty,\infty}}$ for the rotational part and $\sigma_{p_{\infty,\infty}}$ for the point-displacement part. The maximum 2–norms of the rotational and point-displacement parts are denoted by $\sigma_{r_{\infty,2}}$ and $\sigma_{p_{\infty,2}}$, respectively. In order to compute $\sigma_{r_{\infty,2}}$ and $\sigma_{p_{\infty,2}}$, one may proceed by vertex enumeration, i.e., compute the 2–norms associated with each vertex and retain the largest. Thus, as the first step, the coordinates of these vertices should be obtained, and to do so, the above constraint is formulated as follows:

$$\mathbf{L}\Delta \mathbf{x} \preceq \mathbf{1}_{12}, \qquad (3)$$

in which, $\mathbf{L} \equiv [\,\mathbf{K}^T - \mathbf{K}^T\,]^T$, $\preceq$ denotes the componentwise inequality, where $\mathbf{1}_{12} \equiv [1\ 1\ \cdots\ 1]^T \in \mathbb{R}^{12}$. Each row of Eq. (3) can be regarded as a hyperplane containing a facet of the constraint polyhedron. The vertices of this zonotope are determined by the intersection points of different combinations of six independent rows of Eq. (3). Each vertex can be obtained by multiplying the

vector $\mathbf{1}_6$ with the inverse of the matrix formed by the corresponding independent rows. This zonotope has 2^n vertices and is symmetrical about the origin. Thus the computation of the kinematic sensitivity requires only the examination of half of the vertices.

As a case study, let us consider the 3-R$\underline{P}$R parallel mechanism shown in Fig. 1, which in a given posture has the Jacobian matrix [6]

$$\mathbf{K} = \begin{bmatrix} 0.5456 & 0.8380 & 0.0535 \\ -0.8080 & 0.5892 & 0.5892 \\ -0.8588 & -0.5123 & 0.9999 \end{bmatrix}. \tag{4}$$

To obtain $\sigma_{p,\infty,\infty}$ and $\sigma_{p,\infty,2}$, the constraint equation is $\| \mathbf{Kx} \|_\infty \leq 1$. This constraint is equivalent to

$$\begin{bmatrix} 0.5456 & 0.8380 & 0.0535 \\ -0.8080 & 0.5892 & 0.5892 \\ -0.8588 & -0.5123 & 0.9999 \\ -0.5456 & -0.8380 & -0.0535 \\ 0.8080 & -0.5892 & -0.5892 \\ 0.8588 & 0.5123 & -0.9999 \end{bmatrix} \begin{bmatrix} x \\ y \\ \phi \end{bmatrix} \preceq \begin{bmatrix} 1 \\ 1 \\ 1 \\ 1 \\ 1 \\ 1 \end{bmatrix}. \tag{5}$$

The above can be made equivalent to a polyhedron that has eight vertices. Note that this polyhedron is symmetric about the origin, and therefore, it is sufficient to compute half of the vertices $\mathbf{v}_i = (x_i, y_i, \phi_i)$, $i = 1, \ldots, 4$. This can be done by considering four subsystems of three equations. For instance, upon considering the first two equations combined in turns with the the third, the fourth, the fifth and the sixth equation, we obtain the vertices

$$\mathbf{v}_1 = \begin{bmatrix} 0.6189 \\ 0.6706 \\ 1.8752 \end{bmatrix}, \quad \mathbf{v}_2 = \begin{bmatrix} 2.8143 \\ -0.8301 \\ 2.9921 \end{bmatrix}, \quad \mathbf{v}_3 = \begin{bmatrix} 1.6415 \\ 0.0952 \\ 0.4586 \end{bmatrix}, \quad \mathbf{v}_4 = \begin{bmatrix} -0.5539 \\ 1.5959 \\ -0.6582 \end{bmatrix}. \tag{6}$$

The remaining vertices, are merely the opposites of the latter, but they are not required for computing the kinematic sensitivity. According to the definition of the kinematic sensitivity, when $c = \infty$, we have

$$\sigma_{p\infty,\infty} = \max(\max_{i=1,\ldots,8} x_i, \max_{i=1,\ldots,8} y_i) = \max(\max_{i=1,\ldots,4} |x_i|, \max_{i=1,\ldots,4} |y_i|) = 2.8143, \tag{7}$$

$$\sigma_{p\infty,2} = \sqrt{\max_{i=1,\ldots,8} x_i^2 + y_i^2} = \sqrt{\max_{i=1,\ldots,4} x_i^2 + y_i^2} = 2.9342, \tag{8}$$

$$\sigma_{r\infty,\infty} = \sigma_{r\infty,2} = \max_{i=1,\ldots,8} \phi_i = \max_{i=1,\ldots,4} |\phi_i| = 2.9921. \tag{9}$$

As depicted in Fig. 2(a), only four vertices need to be compared in Eqs. (7-9), due to the symmetry of the feasible set. Moreover, this mechanism has only one rotational DOF, and, consequently, $\sigma_{r\infty,\infty} = \sigma_{r\infty,2}$.

2.2 Kinematic sensitivity in the case for which $c = 2$ and $f = \{2, \infty\}$

In [1], the calculation of the kinematic sensitivity using a 2–norm constraint with a 2–norm objective function is discussed in details. The constraint $\| \mathbf{Kx} \|_2 \leq 1$ geometrically describes an
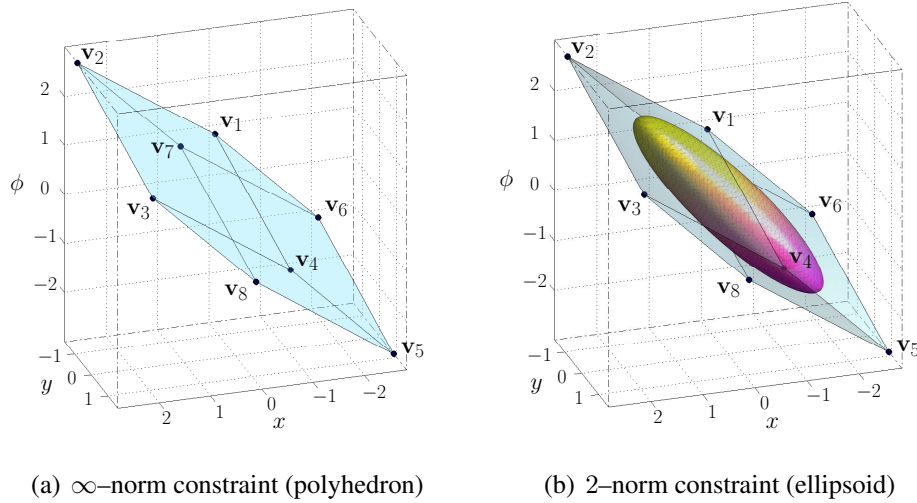
(a) ∞–norm constraint (polyhedron)   (b) 2–norm constraint (ellipsoid)

Figure 2: Kinematic sensitivity constraint based on ∞–norm and 2–norm. The ellipsoid of 2–norm constraint is completely surrounded by the polyhedron of ∞–norm constraint.

ellipsoid in $\mathbb{R}^6$. Let us use the notation as proposed in [7] to represent this ellipsoid, i.e.,

$$\varepsilon(\mathbf{0}_6, \mathbf{K}^T\mathbf{K}) \equiv \{x \in \mathbb{R}^6 \mid (\mathbf{x} - \mathbf{0}_6)^T\mathbf{K}^T\mathbf{K}(\mathbf{x} - \mathbf{0}_6) = 1\}, \tag{10}$$

where, the first argument represents the position of the centre of the ellipsoid. In order to obtain the maximum rotation and point-position kinematic sensitivities, we need to project the constraint ellipsoid $\varepsilon(\mathbf{0}_6, \mathbf{K}^T\mathbf{K})$ on the position and the rotation subspaces, respectively. Directly from [1], we can determine that the projected ellipsoids are coincident to $\varepsilon(\mathbf{0}_3, \mathbf{E}_p)$ and $\varepsilon(\mathbf{0}_3, \mathbf{E}_r)$, respectively, where $\mathbf{E}_p$ and $\mathbf{E}_r$ are given as follows:

$$\mathbf{E}_p = \mathbf{K}_p^T\mathbf{P}_r\mathbf{K}_p \quad , \quad \mathbf{E}_r = \mathbf{K}_r^T\mathbf{P}_p\mathbf{K}_r \tag{11}$$

$$\mathbf{P}_r \equiv \mathbf{1}_{6\times6} - \mathbf{K}_r(\mathbf{K}_r^T\mathbf{K}_r)^{-1}\mathbf{K}_r^T \quad , \quad \mathbf{P}_p \equiv \mathbf{1}_{6\times6} - \mathbf{K}_p(\mathbf{K}_p^T\mathbf{K}_p)^{-1}\mathbf{K}_p^T. \tag{12}$$

Having computed the projections of ellipsoid $\varepsilon(\mathbf{0}_6, \mathbf{K}^T\mathbf{K})$ on rotation and point-position subspaces, we may compute the lengths of their semimajor axes, which yield the corresponding kinematic sensitivities:

$$\sigma_{p2,2} = \sqrt{\| \mathbf{E}_p^{-1} \|_2} = \frac{1}{\sqrt{\min_{i=1,2,3} \lambda_{p,i}}}, \quad \sigma_{r2,2} = \sqrt{\| \mathbf{E}_r^{-1} \|_2} = \frac{1}{\sqrt{\min_{i=1,2,3} \lambda_{r,i}}}, \tag{13}$$

In these relations, $\lambda_{p,i}$ and $\lambda_{r,i}$, $i = 1, 2, 3$, represent the eigenvalues of $\mathbf{E}_p$ and $\mathbf{E}_r$, respectively. The same procedure may be used to compute the maximum error in every direction, x_i, $i = 1, \ldots, 6$, of the Cartesian workspace, resulting from errors bounded by the 2–norm in the joint space ($\| \boldsymbol{\rho} \|_2 \leq 1$). Skipping mathematical details, we obtain the projection of constraint ellipsoid $\varepsilon(\mathbf{0}_6, \mathbf{K}^T\mathbf{K})$ along the axis x_i, which we denote by $\varepsilon(0, E_i)$

$$E_i = \mathbf{k}_i^T\mathbf{P}_{-i}\mathbf{k}_i, \qquad \mathbf{P}_{-i} \equiv \mathbf{1}_{6\times6} - \mathbf{K}_{-i}(\mathbf{K}_{-i}^T\mathbf{K}_{-i})^{-1}\mathbf{K}_{-i}^T, \tag{14}$$

in which, $\mathbf{K}_{-i}$ is the Jacobian matrix $\mathbf{K}$ without its ith column $\mathbf{k}_i$. As $\varepsilon(0, E_i)$ is the projection on the axis, it is not an ellipsoid any more, but rather an interval centred at the origin, with E_i as its inverse squared half-length. According to the definition of the kinematic sensitivities using the 2–norm constraint and the ∞–norm objective function, these indices may be computed as

$$\sigma_{p2,\infty} = \max_{i=1,2,3} d_i, \qquad \sigma_{r2,\infty} = \max_{i=4,5,6} d_i, \tag{15}$$

where $d_i = \frac{1}{\sqrt{E_i}}$ is the farthest distance along the x_i axis.

In order to illustrate the derivation of these values, consider the case study of the 3-R$\underline{\text{P}}$R whose Jacobian matrix is momentarily given by matrix $\mathbf{K}$ of Eq. (4). We wish to compute the kinematic sensitivity based on the 2–norm constraint for this example. From Eq. (12), we have

$$\mathbf{P}_r = \begin{bmatrix} 0.9979 & -0.0234 & -0.0396 \\ -0.0234 & 0.7428 & -0.4365 \\ -0.0396 & -0.4365 & 0.2593 \end{bmatrix}, \qquad \mathbf{E}_p = \begin{bmatrix} 0.4253 & 0.3049 \\ 0.3049 & 1.3012 \end{bmatrix}, \tag{16}$$

$$\mathbf{P}_p = \mathbf{P}_{-3} = \begin{bmatrix} 0.4154 & -0.1988 & 0.4509 \\ -0.1988 & 0.0951 & -0.2158 \\ 0.4509 & -0.2158 & 0.4895 \end{bmatrix}, \qquad E_r = E_3 = 0.3051 \, \frac{\text{m}^2}{\text{rad}^2}. \tag{17}$$

Using Eq. (13), one may derive

$$\sigma_{p2,2} = \sqrt{\| \, \mathbf{E}_p^{-1} \, \|_2} = 1.7418, \qquad \sigma_{r2,2} = \sqrt{\| \, E_r^{-1} \, \|_2} = \frac{1}{\sqrt{E_3}} = 1.8106 \, \frac{\text{rad}}{\text{m}}. \tag{18}$$

As the mechanism has only one rotational DOF, it follows that $\sigma_{r2,\infty} = \sigma_{r2,2}$. In turn, from Eqs. (14), the maximum distance along the x and y axes is obtained as

$$\mathbf{K}_{-x} = \begin{bmatrix} 0.8380 & 0.0535 \\ 0.5892 & 0.5892 \\ -0.5123 & 0.9999 \end{bmatrix}, \quad \mathbf{P}_{-x} = \begin{bmatrix} 0.4520 & -0.4390 & 0.2345 \\ -0.4390 & 0.4264 & -0.2277 \\ 0.2345 & -0.2277 & 0.1217 \end{bmatrix}, \quad \mathbf{E}_x = 0.3538, \tag{19}$$

$$\mathbf{K}_{-y} = \begin{bmatrix} 0.5456 & 0.0535 \\ -0.8080 & 0.5892 \\ -0.8588 & 0.9999 \end{bmatrix}, \quad \mathbf{P}_{-y} = \begin{bmatrix} 0.1587 & 0.3110 & -0.1918 \\ 0.3110 & 0.6095 & -0.3758 \\ -0.1918 & -0.3758 & 0.2317 \end{bmatrix}, \quad \mathbf{E}_y = 1.0826. \tag{20}$$

where, $d_x = 1.6811$ and $d_y = 0.9611$. From Eq. (15), we reach $\sigma_{p2,\infty} = \max(d_x, d_y) = 1.6811$.

2.3 Comparison Between Different Variants of the Kinematic Sensitivity

Figure 3 shows a geometric representation of different versions of the kinematic sensitivity. According to this figure, different kinematic sensitivity measures are related through the following inequalities:

$$\sigma_{\infty,2} \geq \sigma_{\infty,\infty} \geq \sigma_{2,\infty}, \qquad \sigma_{\infty,2} \geq \sigma_{2,2} \geq \sigma_{2,\infty}. \tag{21}$$

There is no such relationship between $\sigma_{\infty,\infty}$ and $\sigma_{2,2}$. According to Fig. 3, if the constraint ellipsoid or polyhedron rotates, the value of $\sigma_{\infty,\infty}$ and $\sigma_{2,\infty}$ would change in consequence while the value
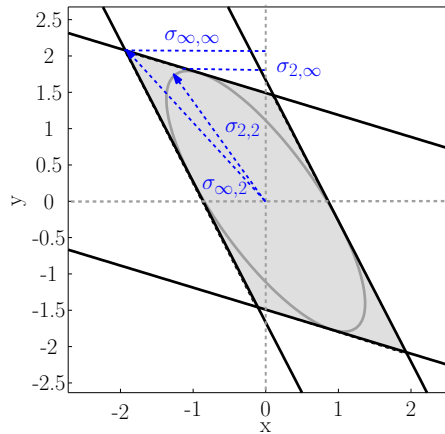
Figure 3: Geometric representation of different variants of kinematic sensitivity in the case of a constrained manipulator.

of $\sigma_{\infty,2}$ and $\sigma_{2,2}$ remain the same. Also, it should be noted that a change in coordinates, although affecting the Jacobian of the mechanism for a given pose, should not affect its kinematic sensitivity index. Because of this frame–invariant requirement, it may be concluded that it is preferable to compute the norm of $\mathbf{x}$ using the 2–norm. Coupling this with the idea proposed by Merlet in [6], according to which the constraint should be defined with the ∞–norm, $\sigma_{\infty,2}$ stands out as the most meaningful index for the calculation of the point–displacement and rotation kinematic sensitivities.

3   KINEMATIC SENSITIVITY IN THE CASE OF REDUNDANT PARALLEL MECHANISMS

Redundant parallel manipulators have been introduced to alleviate some of the shortcomings of fully parallel mechanisms in terms of kinematic properties, such as their large singularity loci [8,9]. In this section, the kinematic sensitivity of redundant planar parallel mechanisms is investigated in order to gain a better understanding of their kinematic properties compared to those of fully parallel mechanisms.

In redundant mechanisms, the number of hyperplanes generated by the ∞–norm constraint increases and further confines the feasible set. As shown in Fig. 4(b), if the redundant rows— corresponding to the redundant limbs—constrain the feasible polyhedron more tightly, they will reduce the mechanism kinematic sensitivities. In redundant mechanisms, the number of vertices of the zonotope generated by the ∞–norm constraint increases. Nevertheless, these vertices can be determined by considering all possible subsets of three independent rows in Eq. (3). It should be noted that some of the intersection points of these triplets of hyperplane constraints lie outside the feasible polyhedron, as depicted in Fig. 4(b). Reaching this step, one should verify whether the obtained point satisfies the remaining inequalities of Eq. (3). If not, then it is not a true vertex.

In order to illustrate the effects of redundancy, consider the above mentioned 3-R$\underline{\text{P}}$R parallel mechanism, whose Jacobian matrix $\mathbf{K}$ is given in Eq. (4). Assume that the legs of the manipulator are all connected at the origin O' of the moving frame, which results in a redundant mechanism that has only two DOFs (planar point-displacements), and, therefore, the associated Jacobian matrix has three rows and two columns. Considering only the first two actuators, ρ_1 and ρ_2, the first-order

(a) non-redundant mechanism constraint, $\sigma_{2,2} = 1.056$ and $\sigma_{\infty,2} = 1.453$

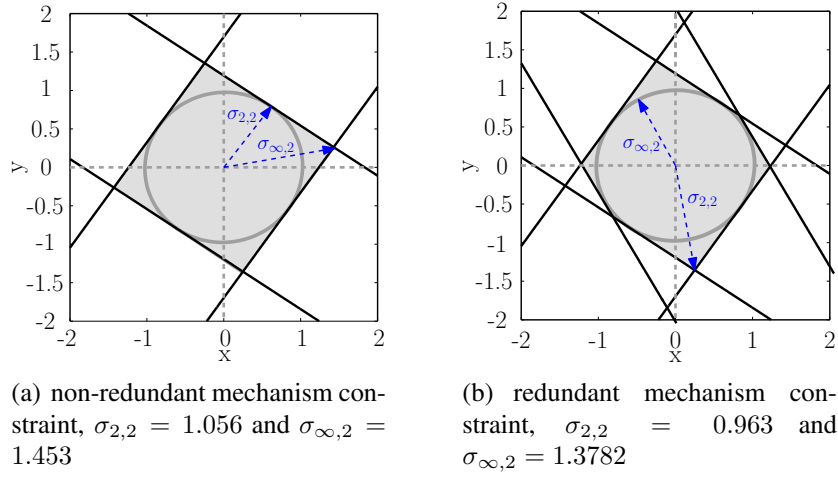(b) redundant mechanism constraint, $\sigma_{2,2} = 0.963$ and $\sigma_{\infty,2} = 1.3782$

Figure 4: ∞–norm and 2–norm constraints, (a) a non-redundant and (b) a redundant mechanism in a given pose. The representations of other indices are omitted to avoid overloading the figure, see Fig. 3 for more information.

kinematics relationship of this mechanism results in

$$\begin{bmatrix} \rho_1, \rho_2 \end{bmatrix}^T = \mathbf{K}_{2\times2}\mathbf{x}, \quad \text{where}, \quad \mathbf{K}_{2\times2} = \begin{bmatrix} 0.5456 & 0.8380 \\ -0.8080 & 0.5892 \end{bmatrix}. \tag{22}$$

In this case, the constraint ellipse is represented by the equation

$$(0.5456x + 0.8380y)^2 + (-0.8080x + 0.5892y)^2 = 1. \tag{23}$$

Figure 4(a) depicts the constraint ellipse and polygon corresponding to the given Jacobian. Assume now that the third limb becomes active, while the pose of the end effector remains unchanged. The Jacobian then matrix takes the following form:

$$\begin{bmatrix} \rho_1, \rho_2, \rho_3 \end{bmatrix} = \mathbf{K}_{3\times2} \begin{bmatrix} x \\ y \end{bmatrix}, \quad \text{where} \quad \mathbf{K}_{3\times2} = \begin{bmatrix} 0.5456 & 0.8380 \\ -0.8080 & 0.5892 \\ -0.8588 & -0.5123 \end{bmatrix}. \tag{24}$$

In this case, the constraint ellipsoid is

$$(0.5456x + 0.8380y)^2 + (-0.8080x + 0.5892y)^2 + (-0.8588x - 0.5123y)^2 = 1. \tag{25}$$

It should be noted that the constraint ellipsoid of a redundant mechanism lies inside the constraint ellipsoid of the non-redundant mechanism obtained by removing some of its legs, and taken in the same posture. Therefore, the kinematic sensitivity is larger or equal to that of the latter. Using the ∞–norm in the constraint leads to a similar conclusion. The number of planes that bound the constraint polyhedron is increased in the case of redundant mechanisms, and the constraint polyhedron becomes smaller or remains the same. Thus, the kinematic sensitivity may either decrease or remain the same in the corresponding redundant manipulator.

From the above it follows that upon transforming a fully actuated mechanism into a redundant one, by adding on limb, one term would be added to the expression defining the constraint ellipsoid which makes the constraint shape smaller. Based on the latter mathematical reasoning, which is based on the 2-norm constraint, one would draw an erroneous conclusion that making a mechanism redundant, would definitely decrease the kinematic sensitivity compared with the one of the corresponding fully actuated mechanism. In fact, in the latter case, the kinematic sensitivity would decrease or remain the same based on the pose and the design parameters of the mechanism. This is coherent with the ∞–norm and makes it more credible than the 2–norm constraint. This reconfirms that the constraint of kinematic sensitivity must be computed using ∞–norm and this is consistent with the conclusion reached in [6].

In order to clarify this issue, assume an exaggerated example, where two of the legs of a redundant 4-R$\underline{P}$R planar parallel mechanism coincide exactly. From intuition, the sensitivity of such a manipulator should be the same as that of the 3-R$\underline{P}$R one obtained by removing one of the redundant legs. In this case, exploring the kinematic sensitivity using a 2–norm constraint in the definition of the kinematic sensitivity, will result in a smaller constraint ellipsoid in the case of the redundant manipulator, and the kinematic sensitivity associated with the latter will be smaller. If the problem is explored using an ∞–norm constraint, however, the redundant hyperplanes in the Cartesian workspace are coincident, just as their corresponding legs. Therefore, the shape and size of the polyhedron constraint remains unchanged, and the kinematic sensitivity is invariant as it should be.

4 KINEMATIC SENSITIVITY OF PARALLEL MECHANISMS WITH DEPENDENT DOF

This section is devoted to the computation of the kinematic sensitivity for planar parallel mechanisms with dependent DOF. In this kind of mechanisms, the Jacobian matrix takes the form

$$\begin{bmatrix} \boldsymbol{\rho} \\ \mathbf{0} \end{bmatrix} = \begin{bmatrix} \mathbf{K}_{\text{actuation}} \\ \mathbf{K}_{\text{constraint}} \end{bmatrix} \mathbf{x}. \tag{26}$$

Failing to consider the equations $\mathbf{K}_{\text{constraint}}\mathbf{x} = \mathbf{0}$ in the kinematic sensitivity analysis leads to an unbounded constraint set $\parallel \mathbf{K}_{\text{actuation}}\mathbf{x} \parallel \leq 1$. This is due to the fact that $\mathbf{K}_{\text{actuation}}$ does not have full-column rank. Hence, the appropriate method for computing the kinematic sensitivity must take into account both the equality constraint $\mathbf{K}_{\text{constraint}}\mathbf{x} = \mathbf{0}$ and the inequality constraint $\parallel \mathbf{K}_{\text{actuation}}\mathbf{x} \parallel \leq 1$.

Assume that one of the actuated joints of the 3-R$\underline{P}$R manipulator is locked, effectively leaving two DOFs of this mechanism, which otherwise has three. Assume that x and y are the important pose parameters for this mechanism. The First–order kinematics of this mechanism may be written as

$$\begin{bmatrix} \rho_1 \\ \rho_2 \\ 0 \end{bmatrix} = \begin{bmatrix} n_{1x} & n_{1y} & (\mathbf{b}_1 \times \mathbf{n}_1) \cdot \mathbf{k} \\ n_{2x} & n_{2y} & (\mathbf{b}_2 \times \mathbf{n}_2) \cdot \mathbf{k} \\ n_{3x} & n_{3y} & (\mathbf{b}_3 \times \mathbf{n}_3) \cdot \mathbf{k} \end{bmatrix} \begin{bmatrix} x \\ y \\ \phi \end{bmatrix}, \tag{27}$$

in which $\mathbf{n}_i = [n_{ix}, n_{iy}, 0]^T$, $i = 1, 2, 3$, stands for the unit vector along the direction of the ith prismatic actuator. Moreover, $\mathbf{b}_i$, $i = 1, 2, 3$, is the vector connecting the centre of the moving platform, O', to point B_i and $\mathbf{k} = [0, 0, 1]^T$ is the vector perpendicular to the end-effector plane.
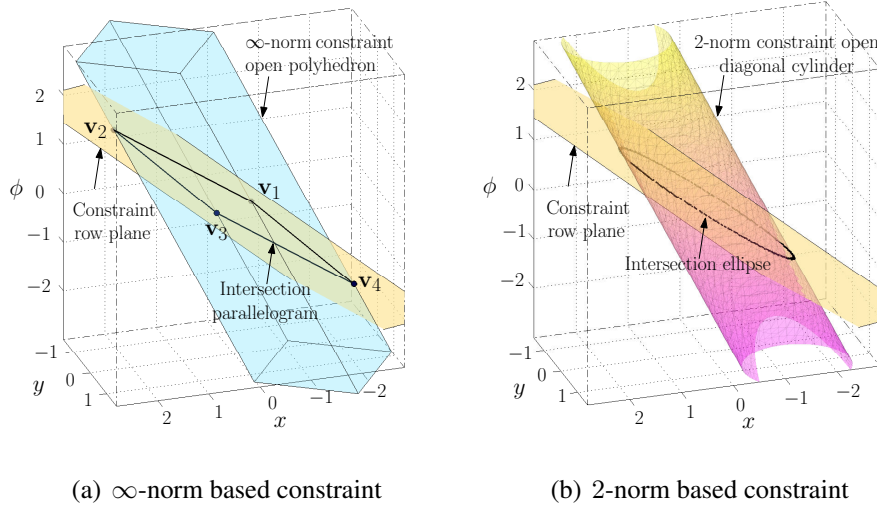
(a) ∞-norm based constraint

(b) 2-norm based constraint

Figure 5: Geometric representation of the kinematic sensitivity constraints for a 3-R$\underline{P}$R parallel manipulator with dependent DOF mechanism, i.e., with a locked actuator.

Figure 5(a) shows the ∞–norm constraint associated with the kinematic sensitivity without considering the constraint row in Eq. (27). Note that this constraint row represents a plane in the space $\mathbb{R}^3$, which is also shown in Fig. 5(a). In order to obtain the kinematic sensitivity, we must compute the intersection of the unbounded zonotope $\parallel \mathbf{K}_{\text{actuation}}\mathbf{x} \parallel_{\infty} \leq 1$ with the constraint row. Figure 5(a) shows the intersections of the kinematic sensitivity constraint and the corresponding constraint row, which is a parallelogram. Now, assume that $\mathbf{K}$ is as in the previous examples which allows to obtain $\sigma_{p_{\infty,\infty}}$ and $\sigma_{p_{\infty,2}}$. The constraint, Eq. (3) can then be written as

$$\begin{bmatrix} 0.5456 & 0.8380 & 0.0535 \\ -0.8080 & 0.5892 & 0.5892 \\ -0.5456 & -0.8380 & -0.0535 \\ 0.8080 & -0.5892 & -0.5892 \end{bmatrix} \begin{bmatrix} x \\ y \\ \phi \end{bmatrix} \preceq \begin{bmatrix} 1 \\ 1 \\ 1 \\ 1 \end{bmatrix}, \quad \text{and} \quad \begin{bmatrix} -0.8588 \\ -0.5123 \\ 0.9999 \end{bmatrix}^T \begin{bmatrix} x \\ y \\ \phi \end{bmatrix} = 0. \tag{28}$$

The feasible polyhedron, (or parallelogram , in this case) has four vertices. Note that this polyhedron is symmetric about the origin, so that it is sufficient to compute a half of the vertices $\mathbf{v}_i = (x_i, y_i, \phi_i)$, $i = 1, 2$. Hence, we obtain

$$\begin{bmatrix} 0.5456 & 0.8380 & 0.0535 \\ -0.8080 & 0.5892 & 0.5892 \\ -0.8588 & -0.5123 & 0.9999 \end{bmatrix} \begin{bmatrix} x_1 \\ y_1 \\ \phi_1 \end{bmatrix} = \begin{bmatrix} 1 \\ 1 \\ 0 \end{bmatrix} \implies \mathbf{v}_1 = \begin{bmatrix} 0.0325 \\ 1.1333 \\ 0.6085 \end{bmatrix}, \tag{29}$$

$$\begin{bmatrix} 0.5456 & 0.8380 & 0.0535 \\ 0.8080 & -0.5892 & -0.5892 \\ -0.8588 & -0.5123 & 0.9999 \end{bmatrix} \begin{bmatrix} x_2 \\ y_2 \\ \phi_2 \end{bmatrix} = \begin{bmatrix} 1 \\ 1 \\ 0 \end{bmatrix} \implies \mathbf{v}_2 = \begin{bmatrix} 2.2279 \\ -0.3674 \\ 1.7253 \end{bmatrix}. \tag{30}$$

The remaining vertices are the opposites of those of Eqs. (29) and (30). The corresponding objec-

tive values are

$$\sigma_{p_\infty,\infty} = \max(\max_{i=1,\dots,4} x_i, \max_{i=1,\dots,4} y_i) = \max(\max_{i=1,2} |x_i|, \max_{i=1,2} |y_i|) = 2.2279, \tag{31}$$

$$\sigma_{p_\infty,2} = \max_{i=1,\dots,4} \sqrt{x_i^2 + y_i^2} = \max_{i=1,2} \sqrt{x_i^2 + y_i^2} = 2.2580, \tag{32}$$

$$\sigma_{r_\infty,\infty} = \sigma_{r_\infty,2} = \max_{i=1,\dots,4} \phi_i = \max_{i=1,2} |\phi_i| = 1.7253. \tag{33}$$

The kinematic sensitivity based on 2–norm constraints may be computed in a similar way when one of the mechanism actuated joints is locked. Figure 5(b) shows the ellipse of the 2-norm constraint obtained from the intersection of the ellipsoidal cylinder $\| \mathbf{Kx} \|_2 \leq 1$ and the plane of the constraint corresponding to the locked joint.

5   KINEMATIC SENSITIVITY AS A GLOBAL PERFORMANCE INDEX

Since the kinetostatic indices generally depend on the pose of the mobile platform, the next step consists in extending them to all the reachable poses of the mechanism. Following the reasoning presented in [10], instead of considering the index I for a specific pose, a global index ζ_I covering the manipulator workspace W is introduced as:

$$\zeta_I = \frac{\int_W I \, dW}{\int_W dW}. \tag{34}$$

Notice that ζ_I tends towards infinity at singular poses when it is applied for $\sigma_{p\infty,2}$ and $\sigma_{r\infty,2}$. Therefore, it is difficult to compare two mechanisms that have at least one singular point in their workspace, as it is not clear whether the integral $\int_W I \, dW$ converges or not. In the case where a dimensional-synthesis method would guarantee the absence of singular poses, then Eq. (34) would hold over the entire workspace, otherwise, however, in general, freeing the whole workspace from all singular poses is impossible, and, consequently, there is a need for a more robust global index. To circumvent this problem, consider the reasoning applied to the condition number in [10]. Point-displacement and rotation sensitivities are bounded between zero and infinity, and hence, their inverse are not helpful over the same interval. As the minimization of the variation of these indices is of interest, the maximization of the inverse of their offshoot is suggested in this paper, i.e., we define

$$\sigma'_{r,2} = \frac{1}{1 + \sigma_{r,2}}, \qquad \sigma'_{p,2} = \frac{1}{1 + \sigma_{p,2}} \qquad \Longrightarrow \qquad 0 \leq \sigma'_{r,2} \leq 1, \quad 0 \leq \sigma'_{p,2} \leq 1 \tag{35}$$

The above indices are well defined, and may be used for optimization purposes.

6   CONCLUSIONS

This paper investigated the interpretation and calculation of different variants of the kinematic sensitivity of planar parallel mechanisms. As a case study, the 3-RPR planar mechanism was analysed and the corresponding kinematic sensitivities were given geometric interpretations. Analytical relationships to compute each of the variations were obtained and discussed. Moreover, the calculation of the kinematic sensitivity in the case of redundant and dependent-DOF planar parallel

mechanisms are investigated, and some new observations are reported. Finally, the kinematic sensitivity is extended to be considered as a global performance index for optimization purposes. The principles of this paper can be applied equally well to the other types of parallel mechanisms, such as the Stewart–Gough platform. Ongoing work includes the development of a robust approach to obtain representative global kinematic sensitivity for optimization purposes.

REFERENCES

[1] P. Cardou, S. Bouchard, and C. Gosselin. Kinematic-Sensitivity Indices for Dimensionally Nonhomogeneous Jacobian Matrices. *IEEE Transactions on Robotics and Automation*, 26(1):166–173, 2010.

[2] N. Binaud, S. Caro, and P. Wenger. Sensitivity Comparison of Planar Parallel Manipulators. *Mechanism and Machine Theory*, 45(11):1477 – 1490, 2010.

[3] T. Yoshikawa. Manipulability of Robotic Mechanisms. *The International Journal of Robotics Research*, 4(2):3, 1985.

[4] W. A. Khan and J. Angeles. The Kinetostatic Optimization of Robotic Manipulators: The Inverse and the Direct Problems. *Journal of Mechanical Design*, 128(1):168–178, 2006.

[5] L. J. Stocco, S. E. Salcudean, and F. Sassani. On the Use of Scaling Matrices for Task-Specific Robot Design. *IEEE Transactions on Robotics and Automation*, 15(5):958–965, 2002.

[6] J. P. Merlet. Jacobian, Manipulability, Condition Number, and Accuracy of Parallel Robots. *Journal of Mechanical Design*, 128(1):199–206, 2006.

[7] L. Ros, A. Sabater, and F. Thomas. An Ellipsoidal Calculus Based on Propagation and Fusion. *IEEE Transactions on Systems, Man. and Cybernetics, Part B:Cybernetic*, 32(4):430–442, 2002.

[8] I. Ebrahimi, J. A. Carretero, and R. Boudreau. A Family of Kinematically Redundant Planar Parallel Manipulators. *Journal of Mechanical Design*, 130:062306, 2008.

[9] N. Rakotomanga and I. A. Bonev. Completely Eliminating the Singularities of a 3-DOF Planar Parallel Robot with Only One Degree of Actuator Redundancy. In *Proceedings of the 2010 ASME Design Engineering Technical Conferences, DETC2010-28829*.

[10] C. Gosselin. *Kinematic Analysis, Optimization and Programming of Parallel Robotic Manipulators*. PhD thesis, Department of Mechanical Engineering, McGill University, Montreal, Canada, 1988.